Osteoarthritis and Cartilage (2008) **16,** 708–714

doi:10.1016/j.joca.2007.10.001

Osteoarthritis and Cartilage

International Cartilage Repair Society

OARSI OSTEOARTHRITIS RESEARCH SOCIETY INTERNATIONAL

Solute transport in the deep and calcified zones of articular cartilage[1]

K. P. Arkill Ph.D.* and C. P. Winlove D.Phil.
Biophysics Group, School of Physics, University of Exeter, EX4 4QL, UK

Summary

Objectives: (1) To establish whether the tidemark and calcified cartilage are permeable to low molecular weight solutes, thereby providing a potential pathway for nutrition of cells in the deep cartilage. (2) To investigate transport from the subchondral microcirculation into calcified cartilage in an intact perfused joint and the effects on transport of static loading.

Methods: The permeability of the tidemark and calcified cartilage was investigated in plugs of cartilage and subchondral bone which formed the membrane of a diffusion cell. Transport from the subchondral microcirculation and the effects of load were studied in an intact perfused joint. Both preparations used the metacarpophalangeal joints of mature horses and fluorescein and rhodamine (m.w. ~ 400 Da) were employed as tracers, assayed by quantitative fluorescence microscopy on histological sections.

Results: Calcified cartilage was permeable to both solutes, both from the superficial and the subchondral sides. The effective diffusivity of both solutes was of the order of 9×10^{-9} cm^2 s^{-1}, fivefold less than in the uncalcified cartilage. The calcified zone was heterogeneous, with high uptake of both tracers in the vicinity of the tidemark. The distribution volume of rhodamine B was higher than for fluorescein, consistent with a significant anionic charge in the calcified matrix. Static loading of the intact joint did not affect the transport of rhodamine B but caused a significant decrease in concentration of fluorescein both in the surface and deep zones of the tissue.

Conclusions: Calcified cartilage is permeable to small solutes and the subchondral circulation may make a significant contribution to the nutrition of deep cartilage in the mature horse. Static loading reduces the uptake of small anionic solutes in the intact joint.

Key words: Osteoarthritis, Diffusion, Tidemark, Equine.

Introduction

The principal component of articular cartilage is an extracellular matrix which constitutes over 90% of the tissue volume. The matrix consists of a network of fibrils of Type II collagen, accounting for 60–70% of the dry weight of the tissue whose interstices are filled with a highly hydrated gel of which the principal component is the large, aggregating proteoglycan aggrecan which constitutes 5–15% of the dry weight. Other glycoproteins, lipids and diverse macromolecules make up the remainder of the tissue, but water is quantitatively the major component, amounting to approximately 70% of the total weight of the tissue. The cells are chondrocytes, whose primary function is synthesis and organisation of the matrix molecules that provide the tissue with its requisite mechanical properties (detailed reviews of cartilage structure and function and its constituent macromolecules are found in, for example, Refs. 1–4). The organisation and composition of the tissue vary slightly between species and joints and over the surface of a particular joint. There is also a large and rather consistent change throughout the depth of the tissue. The most notable changes are in the orientation of collagen fibres, from being parallel to the articular surface to perpendicular at the bone interface and in the mineralisation of the deepest region in the form of crystals of various calcium salts. The calcified cartilage is separated from the overlying cartilage by the tidemark, a zone approximately 3 μm in thickness, whose composition and organisation are still incompletely characterised[5]. The lower boundary is known as the cement line, which marks a change in collagen type and fibre orientation[6]. The calcified cartilage and its boundary structures are thought to act as a mechanical coupling and buffer between the poroelastic cartilage and bone, though this view has been questioned by some authors[7].

The present work concerns the transport of solutes into and through cartilage. Cartilage is avascular, but essential nutrients and signal molecules must be delivered to the chondrocytes and metabolites removed at the rates necessary for cellular survival. Often driven by hypotheses relating impaired nutrition to the development of osteoarthritis, a significant body of research has been undertaken on the permeability of the cartilage matrix to water and solutes. It has been established that, especially for smaller solutes, transport generally occurs by diffusion, driven by gradients in chemical potential[8–10]. The relationships of transport to matrix structure have been investigated in tissue, in model systems and theoretically (reviewed in e.g., Ref. 11). The proteoglycans, defining the "small pore network" of the matrix, are the major determinant of both the distribution and diffusivity of solutes. They have little effect on the diffusivity and distribution of small neutral solutes, but because of their high anionic charge density interact strongly with small ions. For large molecules such as proteins there is a large steric interaction. The magnitude of this effect is dependant on the

[1]Grant support: The Coote Bequest.
*Address correspondence and reprint requests to: Dr K. P. Arkill, Biophysics Group, University of Exeter, School of Physics, Exeter EX4 4QL, UK. Tel: 44-1392-264092; Fax: 44-1392-264111; E-mail: k.p.arkill@ex.ac.uk
Received 16 February 2007; revision accepted 1 October 2007.

shape and size of the solute, but for albumin, one of the best characterised solutes, diffusivity in cartilage is an order of magnitude lower than in free solution and its partition coefficient (the fraction of tissue water available to the solute) is less than 0.01[12,13]. Convective transport induced by cyclic compressive loading of the cartilage is believed to be important for larger solutes[8], but static load in the absence of convection reduces the rate of transport, probably because of loss of interstitial water[14,15].

In this paper we investigate the solute permeability properties of the calcified cartilage and its associated structures. These appear not to have been previously measured. However, they are important not only to the nutrition of the cells of deep cartilage but also for the understanding of solute exchange between the tissue as a whole and its surroundings. It is well established that solutes can be exchanged between capillaries in the synovial membrane and the articular surface *via* the synovial fluid. Whether this is adequate to meet the needs of the deep tissue or is supplemented by transport from the bone microcirculation into the deep cartilage remains controversial. An established view is that the endplate of the bone is permeable in foetal and immature animals, but is sealed at skeletal maturity[1,16]. This view is based on morphological evidence and on rather limited tracer studies. The latter investigations have employed relatively insensitive techniques such as visual estimation of coloured dye uptake[17] or electrochemical detection of hydrogen[18]. In addition, they have been undertaken on small animals in which scaling arguments suggest that transport across the articular surface is more likely to be adequate to meet the needs of the deep tissue.

We therefore re-examined this question, taking advantage of the sensitivity and high spatial resolution offered by quantitative fluorescence microscopy. The first stage of the investigation was to investigate transport across the tidemark into the underlying calcified cartilage using an *in vitro* diffusion cell system. Having thus established that both the tidemark and mineralised cartilage are permeable to low molecular weight solutes we then set out to investigate whether transport occurs from the subchondral microcirculation into the calcified cartilage. For this purpose we developed a preparation of the intact equine forelimb in which both the joint capsule and the subchondral bone could be perfused with fluorescent tracer. Using this preparation we were able to show uptake both in the unloaded joint and in a joint subjected to a static load.

The equine forelimb was chosen for these measurements because of its size and also because fresh tissues could be obtained from skeletally mature animals of a range of known ages. The structures of the uncalcified cartilage, tidemark and calcified cartilage (see Fig. 1) have been described in some detail for this joint[19]. The calcified cartilage constitutes about 20% of the cartilage thickness, which is rather greater than the range 3–8% observed over a number of other species[20]. The tissue develops a range of pathologies resembling those of the human, and thus forms a basis for future studies on abnormal tissues, though we report here only on histologically normal specimens.

Materials and methods

TISSUE PREPARATION

Equine forelimbs cut from the carpus were obtained immediately after death from an abattoir (Potter's, Taunton, UK). The horses were aged at death by experienced staff and legs from horses with obvious lameness were discarded. Where possible, the legs were neither from ponies nor from very large cob types, but because limbs without extensive disease proved to be surprisingly uncommon the principal selection criteria were age and quality of cartilage rather than type of horse. The specimens were from horses between 7 and 11 years old, with no visible damage to the cartilage. A total of eight limbs were used for the diffusion chamber experiments and three for the final intact joint experiments reported here. The limb circulation was perfused with phosphate buffered saline (PBS, pH 7.0) *via* the main medial artery from a 50 ml syringe immediately after death. Once the outflow was free of blood the limbs were placed in a cool box for transport to the laboratory.

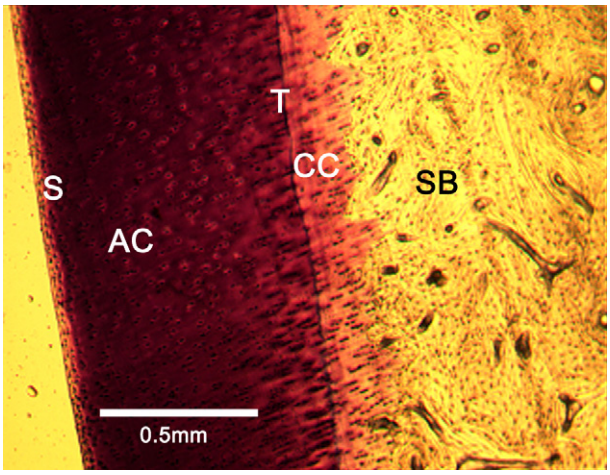

Fig. 1. A cross-section of demineralised metacarpal articular cartilage stained with toluidine blue. AC: articular cartilage, S: articular surface, T: tidemark, CC: calcified cartilage and SB: subchondral bone.

TRACER PREPARATION

Four low molecular weight tracers were employed in this study. Rhodamine B base (Sigma, MW 443, cationic) and rhodamine B (Sigma, MW 479, neutral but polar) have excitation/emission wavelengths of 545/562 nm. Fluorescein (Sigma, MW 332, slightly anionic) and fluorescein sodium salt (Na-fluorescein, Sigma, MW 376, highly anionic) have excitation/emission wavelengths of 494/513 nm. All were dissolved in PBS (pH 7.0). The concentrations of tracer were sufficient to give a good signal compared with tissue autofluorescence but low enough not significantly to change the osmotic balance.

DIFFUSION CHAMBER MEASUREMENTS

The diffusion chamber was purpose made. One side of the chamber contained the tracer solution in contact with the superficial surface of the sample. The other side provided a reservoir of PBS to ensure that the bone remained moist (Fig. 2).

Cartilage plugs, 10 mm in diameter, were prepared using a hole-saw held perpendicular to the surface of the metacarpal distal condyle cartilage, and cut from the subchondral bone using a jeweller's saw leaving a 1 mm layer of subchondral bone attached. The plugs were taken from the weight bearing surface of the phalangeal articulation[21] for consistency with the intact limb experiments. To investigate transport into the calcified layer from the superficial side the overlying articular cartilage was carefully removed using a scalpel to leave only a layer approximately 50 μm thick. In this preparation the tidemark remained intact but the long incubation time required to equilibrate the full thickness of the cartilage was eliminated.

The bone plug was sealed into the diffusion chamber using a quick setting epoxy (Permabond™) at the edges. Care was taken to ensure that the glue did not spread over the surface yet still formed a complete seal. The incubation solution was then introduced into one side of the diffusion chamber in contact with the uncalcified cartilage. Cling film and then aluminium foil were placed over the whole chamber to maintain humidity and minimise photobleaching. Incubation was performed at 4°C using PBS containing fluorescein (0.064 mg/ml) and rhodamine B base (0.064 mg/ml) for 2 h, 5 h and 17 h and 115 h. The lower limit was set as that below which the time required to dismantle the cell and prepare sections for analysis became significant, and the longest time was sufficient for equilibration of the tissue.

INTACT LIMB EXPERIMENTS

At the laboratory the main medial artery and one of the principal veins of the forelimb were exposed by dissection just above the joint capsule and

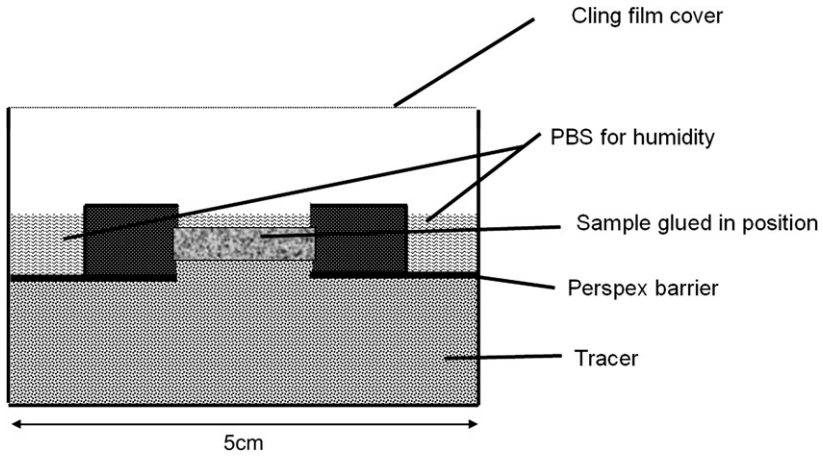

Fig. 2. A diagram of the diffusion chamber.

cannulated. Tourniquets were applied above the cannulation site and around the proximal phalanx to minimise the volume of tracer required. The medial artery was perfused from a Marriot flask providing an inlet pressure of 150 cm water relative to the venous outlet, chosen to be within the physiologically normal pressure range. The limb was perfused with PBS until a steady flow had been achieved and the perfusion solution was then changed to one containing rhodamine B base (0.016 mg/ml). After a perfusion period of 1.5 h the perfusion circuit was disconnected. This perfusion time was chosen in the light of pilot experiments as one at which the concentration profiles from the articular and chondral surfaces did not overlap with each other. The joint was then opened and cartilage–bone plugs 5×5 mm by 2–3 mm deep were rapidly excised, using a jeweller's saw, from the phalangeal articulation surface. This surface was selected as the principal weight bearing surface of the joint under the loading conditions described below[21]. The plugs were wrapped in cling film and frozen in the freezing microtome (Cryocut E, Leica) to -22°C. One excised plug was re-incubated in the perfusion solution for 110–115 h to determine the equilibrium tracer distribution.

LOADING EXPERIMENTS

In a further series of experiments the perfused limb was mounted in a loading rig. The sole of the foot rested on a base plate and a pin running through the shaft of the third metacarpal running parallel to the long axis was loaded to 1500 N by a hydraulic ram. The loaded limb was perfused with PBS containing Na-fluorescein and rhodamine B (0.1 mg/ml) for 1.5 h. The contralateral limb was used as the unloaded control.

QUANTIFICATION OF TRACER DISTRIBUTION

The method of determining tracer intensity profiles has been described in detail previously[13]. From each tissue plug 5–9 transverse frozen sections 20 μm thick, containing cartilage, the calcified zone and a thin layer of bone, were prepared. The sections were taken from the centre of the plug approximately 100 μm apart. The sections were brought to room temperature between glass slides to prevent distortion and dehydration and were examined using a 5× objective under epi-illumination (Leica Aristoplan microscope equipped with I3 and N.2.1 filters). Sample orientation and focussing were performed under low power transmitted white light illumination to avoid photobleaching. 24-bit colour digital images were acquired using a video camera (JVC KY-5F55B) and Image grabber PC software (Acquis Bio, Synoptics Ltd). The camera provided a theoretical pixel resolution of 1.27 μm.

Representative sections from each experiment were extensively washed in PBS before analysis to determine irreversible binding.

Quantification of tracer distribution was performed using a purpose written program (Multiview, developed by Dr CG Phillips, Centre for Biological and Medical Systems, Imperial College, London). Fluorescence intensity profiles were taken along a band 50 μm wide through the full depth of the tissue in the centre of the sections to avoid edge effects. In the *in situ* experiments profiles were taken above filled microvessels (see Fig. 3) which showed as hotspots of intensity. Corrections were made for non-uniformity of illumination and tissue autofluorescence at the rhodamine and fluorescein wavelengths, as determined from plugs of tissue which had not been exposed to fluorophore. In the dual tracer experiments the cross-over of fluorescence from one tracer at the wavelength used to assay the other was measured and found to be negligible. The autofluorescence was non-uniform through the depth of the tissue and the autofluorescence correction was performed locally. Due to the sections being the full depth there was some variation in cartilage thickness, the correction and comparison of tracer distribution between sections were performed first with tissues aligned at the surface for analysis of the surface and mid zone distribution, and then again with the tidemarks aligned for analysis of the distribution in the deep zones. The profiles from the diffusion chamber experiments were aligned at the tidemark.

As in our previous work[13], the intensity profiles were fitted to the solution of the one-dimensional diffusion equation for an infinite source[22]:

$$C(x,t) = C(x,\infty)\mathrm{erfc}(x/(2\sqrt{(Dt)})) \quad (1)$$

where erfc is the complementary error function the effective diffusivity, D, is as a simple measure of the effective transport rate. In implementing this equation we assume the activity coefficients to be unity and fluorescence intensity to be proportional to the fluorophore content of the sampling volume, after subtraction of tissue autofluorescence, $I(x,0)$. The available space for the fluorophore in the sampling volume is defined as the equilibrium intensity, $[I(x,\infty) - I(x,0)]$, and so the effective chemical potential of the fluorophore can be written as $C(x,t) = [I(x,t) - I(x,0)]/[I(x,\infty) - I(x,0)]$, where $I(x,\infty)$ is taken as the value attained after 115 h incubation. Fitting of the experimental data was performed using KaleidaGraph™ 3.52.

Because we found that in the calcified cartilage effective solute diffusivity was lower than in either uncalcified cartilage or subchondral space a second 'sink' diffusion model was also applied. Depending on the direction of transport, one of the latter compartments acted as a source and the other as an effectively infinite sink. To analyse these situations we used the series solution given by Crank[23].

$$C = C_0(1 - (x/L)) - (2/\pi)\sum_{n=1}^{\infty}\sin(nx\pi/L)\exp(-(Dn^2\pi^2 t/L^2))/n \quad (2)$$

where L is the thickness of the calcified zone and n is an integer. This model assumes a constant concentration at $x = 0$, and a constant, zero, concentration at $x = L$. For the time scales involved and the limited accuracy of the data we fitted only the first term of Eq. (2).

Results

We first present the results of measurements of the transport properties of calcified cartilage as determined in the diffusion cell and then describe tracer uptake in the perfused forelimb preparation.

SOLUTE TRANSPORT IN CALCIFIED CARTILAGE

In the diffusion chamber preparation tracer uptake in the thin layer of remaining uncalcified cartilage was much greater than that in the calcified zone. In the calcified zone the distribution of all tracers was non-uniform through

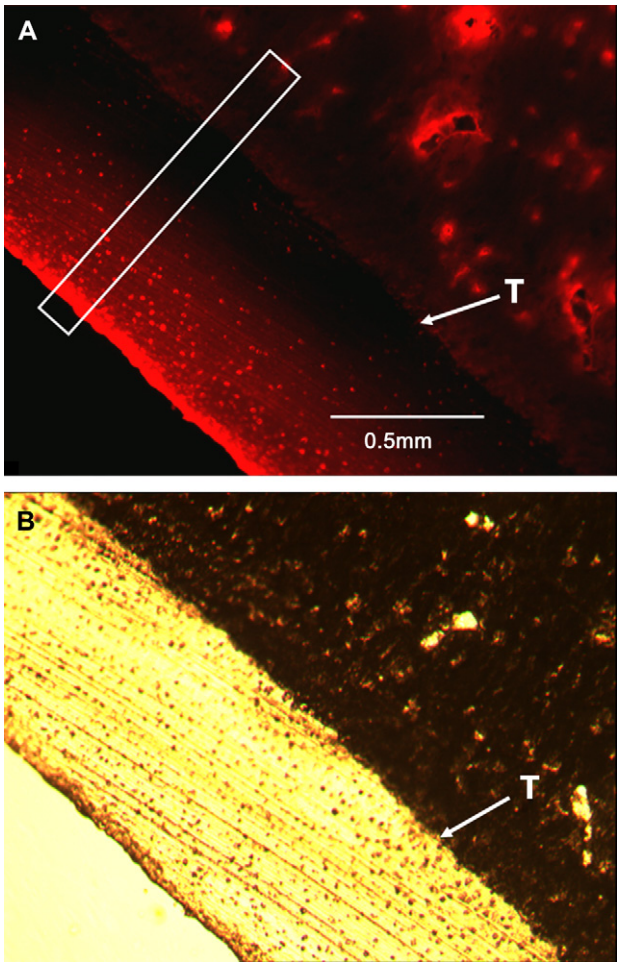

Fig. 3. A representative section of metacarpal articular cartilage from an intact joint perfused with rhodamine B base. The tidemarks are labelled (T). (A) Fluorescence image of rhodamine B base, showing the region from which an intensity profile was constructed. (B) Transmitted white light image of the same area.

the depth of the tissue even after 115 h of incubation (Fig. 4), and did not change significantly with longer incubation times. This distribution was therefore taken to reflect the available space within the tissue. The equilibrium intensity fell over the first 50 μm, but then remained relatively constant. This was particularly noticeable for rhodamine B base for which the equilibrium intensity was almost twofold higher than for fluorescein. Since the tracers are of similar molecular weight we presume that this behaviour reflects electrostatic interaction of the cationic rhodamine with anionic fixed charges in the calcified cartilage. The shape of the profile therefore suggests that the fixed charge density is particularly high in the vicinity of the tidemark.

Using the equilibrium data to scale the tracer uptake intensity at shorter incubation times (so that the values represent the concentration of tracer in the available space at each location) results in the distribution profiles shown in Fig. 5. At all times the tracer concentration was uniform over the first 50–75 μm of calcified cartilage, but thereafter the concentration fell with depth through the tissue. This behaviour is consistent with the existence of a superficial zone in which diffusivity is relatively high.

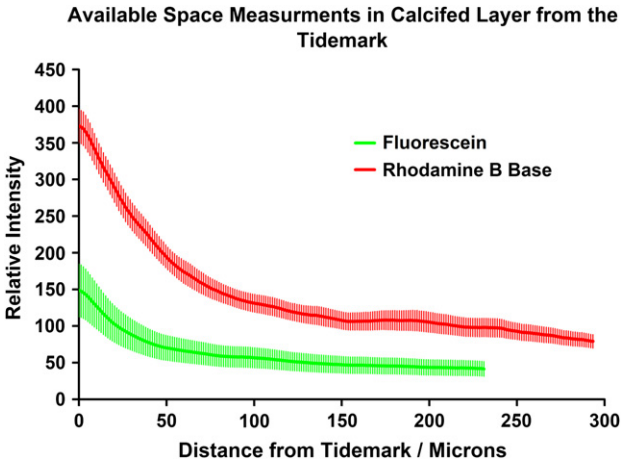

Fig. 4. The equilibrium intensities (115 h) of tracer in the calcified cartilage in diffusion chamber experiments. The intensity profiles for fluorescein ($n = 6$) and rhodamine B base ($n = 15$) and scaled by the concentration of tracer in the incubation medium as described in the text. Standard error bars are shown for each profile.

Using the two diffusion models to fit the mean concentration data the best was obtained with the sink model [Eq. (2)]. The effective diffusion coefficient was $(9.5 \pm 1.2) \times 10^{-9}$ cm^2 s^{-1} for rhodamine B base and $(9.8 \pm 1.3) \times 10^{-9}$ cm^2 s^{-1} for fluorescein at 2 h. At 5 h the coefficient dropped by a factor of three for the positively charged rhodamine B base and by a factor of 1.5 for fluorescein. At 17 h the diffusion coefficient for fluorescein fell further again but rhodamine B base was too close to equilibrium to obtain a reliable estimate.

Washout experiments revealed that only rhodamine B bound irreversibly to the matrix, particularly in the vicinity of the tidemark.

SOLUTE TRANSPORT IN THE INTACT JOINT

In the unloaded joint *en face* examination of the cartilage surface after perfusion revealed fluorophore over the whole joint, though the cortical and the sagittal ridges were noticeably less intensely stained. It was impossible to establish by inspection whether the tracer was in the cartilage or in the subchondral capillaries. However, preliminary experiments showed that the concentration profiles in cartilage did not vary with position so the heterogeneities must reflect regional differences at the level of subchondral microcirculation.

For the present investigation plugs for the construction of distribution profiles were taken from the dorsal condyle, an area of higher uptake. Tracer was evident in the capillaries of the subchondral circulation and in the surrounding matrix.

Figure 6(A) shows the mean intensity profiles from sections aligned at the articular surface, corrected for available space as described above. After 1.5 h of perfusion tracer was present in the synovial fluid and penetrated the cartilage surface. The intensity was uniform over the first 30–50 μm of tissue but it fell through the mid and deep zones of cartilage, becoming undetectable approximately 100 μm before the tidemark. The diffusion model [Eq. (1)] gives an apparent diffusion coefficient for rhodamine B base for transport across the articular surface of $(3.7 \pm 0.3) \times 10^{-8}$ cm^2 s^{-1}. This is consistent with measurements in excised plugs[13], indicating that transport into the

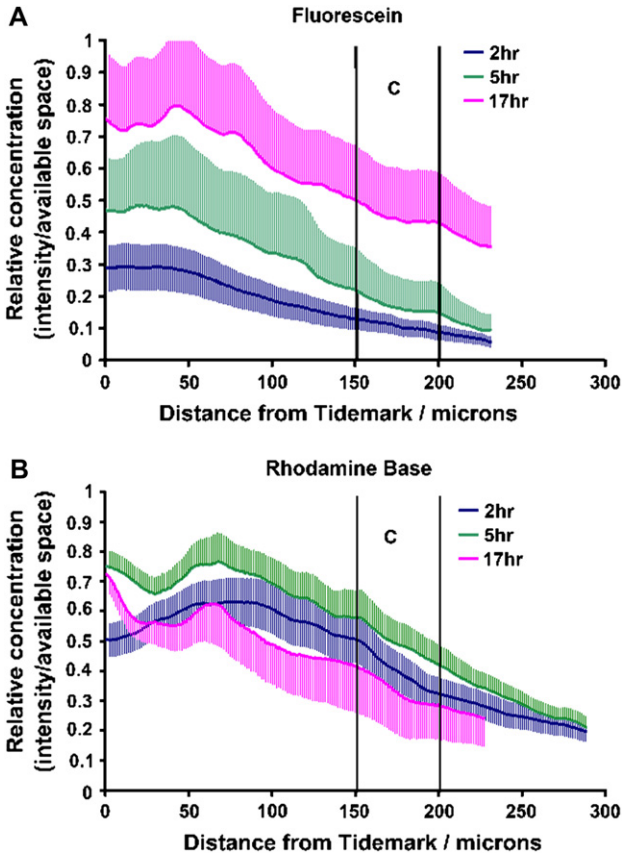

Fig. 5. The distribution of tracer in the calcified zone in diffusion chamber experiments for different incubation times. At each point the concentration is scaled by the equilibrium intensity, shown in Fig. 4, as described in the text. (A) Fluorescein (2 h incubation: $n=5$, 5 h: $n=5$ and 17 h: $n=6$). (B) Rhodamine B base (2 h: $n=8$, 5 h: $n=7$, and 17 h: $n=5$). Distance is measured from the tidemark and the approximate position of the cement line is indicated (C). Standard error bars are shown for each profile.

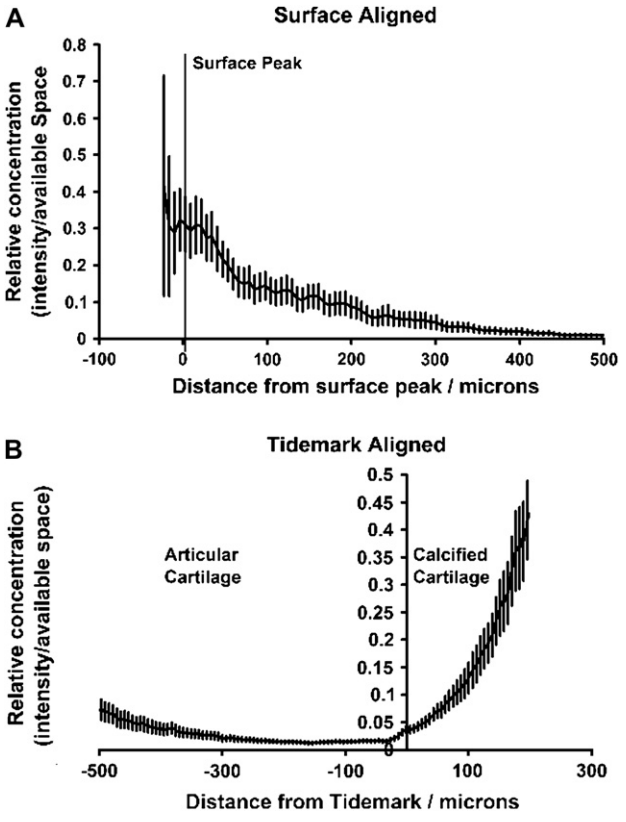

Fig. 6. Concentration profiles (relative to equilibrium concentration) after a 1.5 h rhodamine B base perfusion of the intact joint. (A) Mean profiles aligned at the surface. Positive distance represents depth below the articular surface ($n=26$). (B) Mean profiles aligned at the tidemark ($n=31$). Standard error bars are shown.

joint space is not a rate limiting process in surface uptake even in the immobile joint.

To analyse the distribution in the deep tissue the intensity profiles were aligned at the tidemark, giving the mean distributions shown in Fig. 6(B). There was a significant amount of tracer in the calcified cartilage, the gradient falling from the bone towards the tidemark, indicating that entry was from the subchondral microcirculation. The intensity profiles could adequately be described either by the simple diffusion model [Eq. (1)] or the 'sink' diffusion model [Eq. (2)] giving apparent diffusion coefficients of $(8.2 \pm 0.7) \times 10^{-9}$ cm^2 s^{-1} and $(7.5 \pm 0.4) \times 10^{-9}$ cm^2 s^{-1}, respectively. This is a factor of five less than in the unmineralised articular cartilage, but comparable to that measured in the diffusion cell.

EFFECTS OF LOADING

The concentration profiles in the loaded joints were qualitatively similar to those described above, with uptake from both the articular and subchondral surfaces. However, there were quantitative differences in uptake from both interfaces. These differences were investigated using paired limbs, one loaded and the other unloaded. The limbs were perfused with a mixture of Na-fluorescein and rhodamine B to investigate possible effects of solute charge.

Figure 7 shows the distributions of both tracers, in unloaded and loaded specimens at the articular surface. There was no effect of load on the distribution of rhodamine B. In contrast, for Na-fluorescein the relative concentration decreased under load from 0.6 to 0.2. The profiles were similar in shape to those previously reported in excised plugs[13] except that the uniform zone in the surface to mid layer is thicker in both the loaded and unloaded joints.

Figure 8 shows the effects of loading on transport by the subchondral route. This showed a similar pattern to transport across the articular surface, with no change in rhodamine B uptake, but a reduction in fluorescein uptake.

Discussion

We employed low molecular weight tracers in our investigations both because they are likely to suffer minimal steric exclusion from the extracellular matrix and so offer the greatest sensitivity for detection in the mineralised tissue and also because they are comparable in physical properties to a range of nutrients and signal molecules important for chondrocyte metabolism. Before discussing the physiological significance of our observations we should note that although the transport rates of various tracers were parameterised by the calculation of an effective diffusion coefficient, the time dependence of the measured quantities reveals an inadequacy in the models employed. This could arise from neglect of processes such as matrix binding of the tracer or

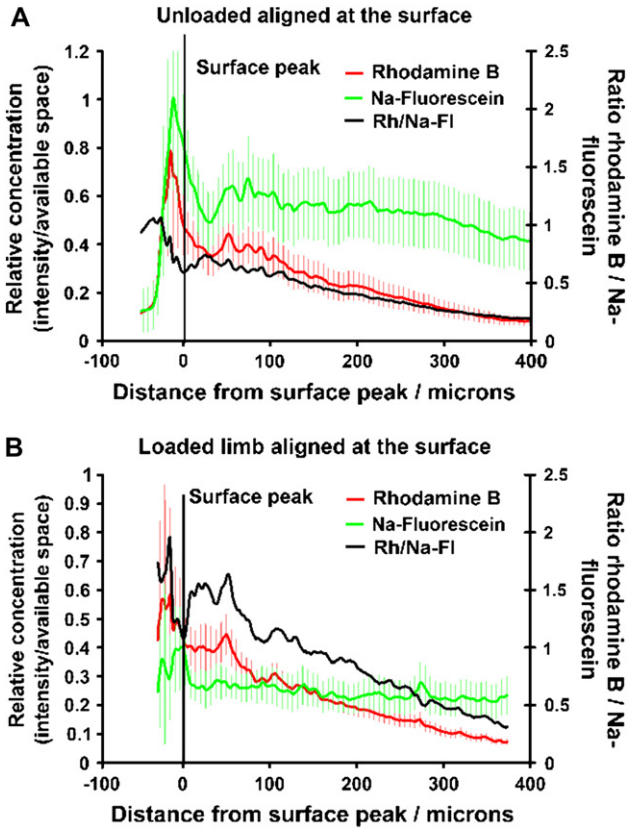

Fig. 7. Concentration profiles after 1.5 h perfusion of the intact joint Na-fluorescein and rhodamine B (0.1 mg/ml). Profiles (scaled by equilibrium concentration) are aligned at the surface peak. Positive distance represents depth below the articular surface. (A) Unloaded joint ($n=7$). (B) Loaded joint ($n=7$). The ratio of rhodamine B (Rh) to Na-fluorescein (Na-Fl) is plotted on the second axis. Standard error bars are shown.

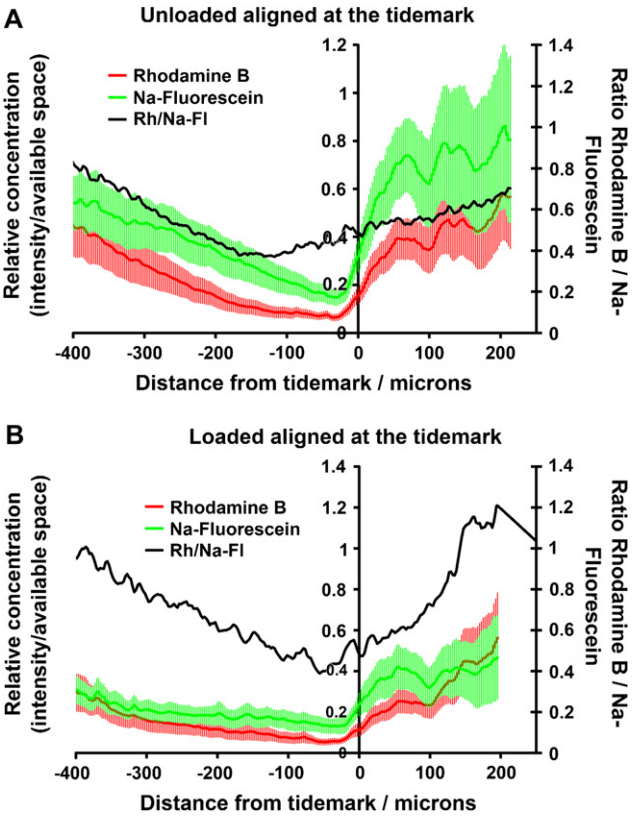

Fig. 8. Data from the experiment described in Fig. 7, but with concentration profiles aligned at the tidemark. (A) Unloaded joint ($n=8$). (B) Loaded joint ($n=8$). The ratio of rhodamine B (Rh) to Na-fluorescein (Na-Fl) is plotted on the second axis. Standard error bars are shown.

from the structural heterogeneity of the tissue as noted by previous authors[12,13,23]. The coefficients should therefore be considered only as comparators of transport rates.

The experiments on excised plugs of tissue demonstrated clearly that, in contrast to previous reports[17,18], the tidemark and mineralised cartilage are permeable to low molecular weight solutes. Though the effective diffusion coefficients are approximately fivefold lower than those in mid-articular cartilage, the short diffusion distance between the cells of the calcified layer and the subchondral microcirculation compared with that from the articular surface means that the former may be important in the nutrition of the deep tissue. The permeability of the calcified cartilage also suggests the possibility of exchange, in either direction, of cytokines, signal molecules and the various substrates required for tissue remodelling between cartilage and subchondral bone. There is current interest in the interplay between bone and cartilage in the development of diseases such as osteoarthritis and osteoporosis[24] and our results suggest that in addition to biomechanical interactions, biochemical interactions should also be considered.

The deep cartilage proved to be heterogeneous through its depth. The tidemark was permeable to tracers and solute uptake was high in its vicinity. We recently reported a similar effect for albumin and lauric acid[13]. Whether this arises because of a larger available volume or because of reversible binding to molecules specific to the tidemark region it was not possible to establish. Only the rhodamine B showed irreversible binding. The shape of the intensity profiles also revealed that the uppermost 50–75 μm of the calcified cartilage has a higher permeability than the deeper region. Again, this could reflect reversible binding.

On a macroscopic scale there was considerable variation of the tracer content in the subchondral microcirculation over the joint surface. The thickness and collagen organisation of the cartilage also vary over the joint surface[25] and these variations have been linked to the pattern of joint loading and pre-disposition to disease[21]. It is a task for the future to correlate these observations. There was also heterogeneity at the microscopic scale, but this was quickly smoothed out in the tissue and no significant spatial variations in uptake by the cartilage could be resolved.

The pathways of transport from the subchondral circulation are not clear. A number of authors have suggested that the bony capsule around the capillaries is closed[16], but a more recent study on human tissue describes channels between subchondral bone and uncalcified cartilage[26]. Such structures might be expected to give a more heterogeneous pattern of uptake in the calcified zone than we observe, but it is difficult to relate histological appearance with permeability and this should be a target for future research.

Static loading did not affect the uptake of a small neutral solute but reduced transport of an anionic probe. This

behaviour is consistent with previous studies on excised tissues showing that water was expressed, having only a marginal effect on the neutral solute, but increasing fixed charge density and thereby electrostatic exclusion[9,27,28], but that transport *via* the subchondral route was also affected was a more unexpected result. Whether it reflects consolidation of the tissue of the deep zone or compression of the subchondral vasculature is an important question for further research.

References

1. Stockwell RA. Biology of Cartilage Cells. Cambridge: Cambridge University Press; 1979.
2. Muir H. Cartilage structure and metabolism and basic changes in degenerative joint disease. Aust N Z J Med 1978;8:1–5.
3. Mow V, Lai WM. Mechanics of animal joints. Annu Rev Fluid Mech 1979; 11:247–88.
4. Ratcliffe A, Mow V. Articular cartilage. In: Comper WD, Ed. Extracellular Matrix. Amsterdam: Harwood Academic Publishers; 1996;vol. 1: 235–302.
5. Redler I, Mow VC, Zimmy ML, Mansell J. The ultrastructure and biomechanical significance of the tidemark of articular cartilage. Clin Orthop Relat Res 1975;112:357–62.
6. Green WT, Garland MN, Eanes ED, Sokoloff L. Microradiographic study of the calcified layer of articular cartilage. Arch Pathol (Chic) 1970;90: 151–8.
7. Mente PL, Lewis JL. Elastic modulus of calcified cartilage is an order of magnitude less than that of subchondral bone. J Orthop Res 1994;12: 637–47.
8. Ohara BP, Urban JPG, Maroudas A. Influence of cyclic loading on the nutrition of articular cartilage. Ann Rheum Dis 1990;49:536–9.
9. Garcia AM, Frank EH, Grimshaw PE, Grodzinsky AJ. Contributions of fluid convection and electrical migration to transport in cartilage: relevance to loading. Arch Biochem Biophys 1996;333:317–25.
10. Garcia AM, Lark MW, Trippel SB, Grodzinsky AJ. Transport of tissue inhibitor of metalloproteinases-1 through cartilage: contributions of fluid flow and electrical migration. J Orthop Res 1998;16: 734–42.
11. Gribbon P, Maroudas A, Parker KH, Winlove CP. Water and solute transport in the extracellular matrix: physical principles and macromolecular determinants. In: Reid RK, Rubin K, Eds. Connective Tissue Biology: Integration and Reductionism. London: Portland Press; 1998:95–123.
12. Maroudas A. Transport of solutes through cartilage: permeability to large molecules. J Anat 1976;122:335–47.
13. Arkill KP, Winlove CP. Fatty acid transport in articular cartilage. Arch Biochem Biophys 2006;456:71–8.
14. Torzilli PA, Dethmers DA, Rose DE, Schryuer HF. Movement of interstitial water through loaded articular cartilage. J Biomech 1983;16: 169–79.
15. Quinn TM, Kocian P, Meister JJ. Static compression is associated with decreased diffusivity of dextrans in cartilage explants. Arch Biochem Biophys 2000;384:327–34.
16. Clark JM. The structure of vascular channels in the subchondral plate. J Anat 1990;171:105–15.
17. Greenwald AS, Haynes DW. A pathway for nutrients from the medullary cavity to the articular cartilage of the human femoral head. J Bone Joint Surg 1969;51B(4):747–53.
18. Ogata KL, Whiteside A, Lesker PA. Subchondral route for nutrition to articular cartilage in the rabbit. Measurement of diffusion with hydrogen gas *in vivo*. J Bone Joint Surg 1978;60-A:905–10.
19. Martinelli MJ, Eurell J, Les CM, Fyhrie D, Bennett D. Age-related morphometry of equine calcified cartilage. Equine Vet J 2002;34:274–8.
20. Oegema TR, Carpenter RJ, Hofmeister F, Thompson RC. The interaction of the zone of calcified cartilage and subchondral bone in osteoarthritis. Microsc Res Tech 1997;37:324–32.
21. Brama PA, Karssenberg D, Barneveld A, Van Weeren PR. Contact areas and pressure distribution on the proximal articular surface of the proximal phalanx under sagittal plane loading. Equine Vet J 2001;33:26–32.
22. Crank J. The Mathematics of Diffusion. 2nd edn. Oxford: Clarendon; 1975.
23. Torzilli PA, Adams TC, Mis RJ. Transient solute diffusion in articular cartilage. J Biomech 1987;20:203–14.
24. Li B, Aspden RM. Mechanical and material properties of the subchondral bone plate from the femoral head of patients with osteoarthritis and osteoporosis. Ann Rheum Dis 1997;56:247–54.
25. Moger CJ, Barrett R, Bleuet P, Bradley DA, Ellis RE, Green EM, *et al*. Regional variations of collagen orientation in normal and diseased articular cartilage and subchondral bone determined using small angle X-ray scattering. Osteoarthritis Cartilage 2007;15:682–7.
26. Lyons TJ, McClure SF, Stoddart RW, McClure J. The normal human chondro-osseous junctional region: evidence for contact of uncalcified cartilage with subchondral bone and marrow spaces. BMC Musculoskelet Disord 2006;7:52.
27. Quinn TM, Morel V, Meister JJ. Static compression of articular cartilage can reduce solute diffusivity and partitioning: implications for the chondrocyte biological response. J Biomech 2001;34:1463–9.
28. Nimer E, Schneiderman R, Maroudas A. Diffusion and partition of solutes in cartilage under static load. Biophys Chem 2003;106:125–46.